J. Iron Steel Res. Int. (2020) 27:1400–1406
https://doi.org/10.1007/s42243-020-00504-y

ORIGINAL PAPER

Effect of basicity and Al_2O_3 on viscosity of ferronickel smelting slag

Yong-feng Chen[1] · Xue-ming Lv[2] · Zheng-de Pang[3,4] · Xue-wei Lv[3,4]

Received: 10 October 2019 / Revised: 31 March 2020 / Accepted: 1 April 2020 / Published online: 27 October 2020

Abstract
The effect of the Al_2O_3 content and basicity (the molar ratio of MgO to SiO_2) on the viscosity of a SiO_2–MgO–FeO–Al_2O_3–CaO slag was studied to fully understand the smelting process of the ferronickel alloy. Experimental results show that the slag is a mixture of liquid and solid phases at the experimental temperature. The viscosity decreased as the basicity increased and increased as the Al_2O_3 content increased. To determine the effect of the Al_2O_3 content and basicity on the structure of the molten slag, Raman spectroscopy was performed on the slag sample, which was quenched from the high temperature with water. The Raman spectra showed that the fractions of the polymerization structural units decreased significantly as the basicity of the slag increased, resulting in a decrease in the apparent viscosity. However, Al_2O_3 acts as a network former in the slag system, thereby making the slag structure further polymerized and increasing the viscosity.

Keywords Nickel laterite ore · Slag structure · Viscosity · Basicity · Ferronickel smelting slag

1 Introduction

Nickel plays an important role in modern steel manufacturing [1]. It is an essential element in stainless steel, which accounts for 65% of the world's nickel consumption [2–4]. In recent years, the global annual demand for nickel has increased tremendously due to increased stainless steel production, particularly in China [5]. Nickel sulfide and laterite ores are the two main resources for extracting nickel metal. With the continuous consumption of sulfide resources, the use of nickel laterite, which accounts for 70% of the nickel resources in the earth's crust, has drawn increasing attention [6, 7]. China lacks nickel resources and has greatly depended on the import for a long period. The use of low-grade nickel laterite in China is regarded as the main solution to the increasing demand for ferronickel alloys. However, the extraction of nickel from nickel laterite ore is relatively difficult due to the low nickel grade, and nickel exists as an isomorphic substitution in serpentine or goethite [8].

The rotary kiln-electric furnace (RKEF) process is the preferred technology for extracting nickel and iron from nickel laterite. Nevertheless, the RKEF process is characterized by energy intensity as it involves several high-temperature processing steps, such as calcination and pre-reduction at 850–1000 °C in a rotary kiln, followed by smelting at 1500–1600 °C in an electric arc furnace to separate the ferronickel alloy from the SiO_2–MgO slag [9, 10].

Generally, the SiO_2 fraction in nickel laterite is high, approximately 30–50 wt.% [11]. Hence, a certain amount of lime should be added to the slag to achieve good fluidity and desulfurization capacity in the industrial smelting process. As a result, the cost of raw materials and the slag volume increase, and the effective volume of the electric

✉ Xue-ming Lv
lvxueming1114@163.com

Yong-feng Chen
y-f-chen@163.com

Zheng-de Pang
pzdcqu@126.com

Xue-wei Lv
lvxuewei@163.com

[1] Wuhu Xinxing Ductile Iron Pipes Co., Ltd., Wuhu 241000, Anhui, China

[2] Pangang Group Research Institute Co., Ltd., Panzhihua 617000, Sichuan, China

[3] Chongqing Key Laboratory of Vanadium-Titanium Metallurgy and New Materials, Chongqing University, Chongqing 400044, China

[4] College of Materials Science and Engineering, Chongqing University, Chongqing 400044, China

arc furnace decreases, thereby reducing the production capability of the furnace. Small addition or no extra addition of lime can decrease the energy consumption and improve the economic smelting indicators to produce each ton of nickel metal. However, small lime addition may increase the viscosity of the slag and result in poor separation of the metal from the slag. Therefore, it is important to study the feasibility of nickel laterite ore smelting with a low amount of lime. In this study, the effects of the basicity and Al_2O_3 content on the viscosity and slag structure were investigated, and the results can approve the feasibility of the new slagging system with low lime content.

2 Experimental

2.1 Sample preparation

The composition of the slag in this study is based on the chemical composition of the nickel laterite ore used in the industry. The main chemical composition of the laterite ore is shown in Table 1.

It can be observed that the nickel laterite sample has high contents of SiO_2 and MgO. Therefore, the basicity (R) in this study is defined as the molar ratio of MgO to SiO_2. In industrial practice, the partial reduction of the iron oxides has been suggested to improve the grade of nickel. Therefore, the slag system in this study is composed of SiO_2, MgO, FeO, Al_2O_3, and CaO.

The slag was synthesized with analytically pure grade reagents ($\geq$ 99% purity) provided by Shanghai Aladdin Co., Ltd., China. The reagents were weighed according to the specified composition and mixed well to attain homogeneity. The mixtures were melted at 1550 °C for 2 h in a $MoSi_2$ furnace under an Ar atmosphere at a flow rate of 1.0 L min^{-1} in a molybdenum (Mo) crucible. Subsequently, the Mo crucible was placed in a corundum crucible, and a graphite crucible was used as the outer layer to remove the remaining oxygen in the furnace. The Mo crucible was rapidly removed from the furnace chamber, and the slag sample was quickly poured into water after premelting. Afterward, the quenched slag was dried in a muffle furnace and crushed for slag viscosity measurement.

2.2 Experimental scheme

The chemical compositions of the slags investigated in this study are presented in Table 2. The basicity was set from 0.8 to 1.0, and the Al_2O_3 content in the slag varied from 4.0 to 10.0 wt.%.

2.3 Experimental apparatus

In this study, the rotating cylinder method was employed for the viscosity measurement. The electric resistance furnace with a $MoSi_2$ heater used in this study is schematically shown in Fig. 1. The torque was recorded using a rotating Mo spindle connected to a Brookfield digital viscometer (model LVDV-II + Pro, USA). The furnace temperature was controlled using a proportional–integral–derivative (PID) controller. When the temperature reached the experimental temperature, the equilibration time for viscosity measurements was selected as 30 min. The average value of the viscosity data was calculated and recorded. The viscometer was calibrated at room temperature using standard oils of known viscosities (i.e., 0.96, 4.92, and 9.80 poise), and the procedure has been reported in a previous publication at a high temperature with the well-known slag in the literature [12].

The structure of the investigated slag was analyzed by Raman spectroscopy (LabRAM HR Evolution, HORIBA Scientific, France). The Raman spectra of the amorphous samples were obtained at room temperature within 100–1900 cm^{-1} with a 532-nm laser source [13–15].

2.4 Experimental procedure

The quenched slag was heated to 1550 °C and held sufficiently for 3 h under 1.0 L min^{-1} of Ar flow in a Mo crucible to homogenize the slag. Thereafter, the spindle was carefully immersed 5 mm deep into the molten slag and located in the middle of the crucible because slight deviations of the spindle from the central axis can easily produce measurement errors. The viscosity was measured at an interval of every 10 °C from 1460 °C to 1550 °C with an equilibration time of 30 min, and the torque values, which were stabilized for 2 min after the equilibrium time, were measured at a fixed spindle rotation speed (12 r/min). The experiments were repeated to obtain reproducible

Table 1 Chemical composition of nickel laterite ore (wt.%)

Ni	TFe	Cr_2O_3	SiO_2	Al_2O_3	CaO	MgO	P	S	Moisture
1.81	17.87	0.51	34.97	4.75	1.54	13.50	0.005	0.064	16.83

Table 2 Chemical compositions of studied slags

Slag	MgO/wt.%	SiO_2/wt.%	Al_2O_3/wt.%	CaO/wt.%	FeO/wt.%	Basicity
1	30.1	56.4	4.0	1.5	8.0	0.8
2	32.4	54.1	4.0	1.5	8.0	0.9
3	34.6	51.9	4.0	1.5	8.0	1.0
4	33.8	50.7	6.0	1.5	8.0	1.0
5	33.0	49.5	8.0	1.5	8.0	1.0
6	32.2	48.3	10.0	1.5	8.0	1.0

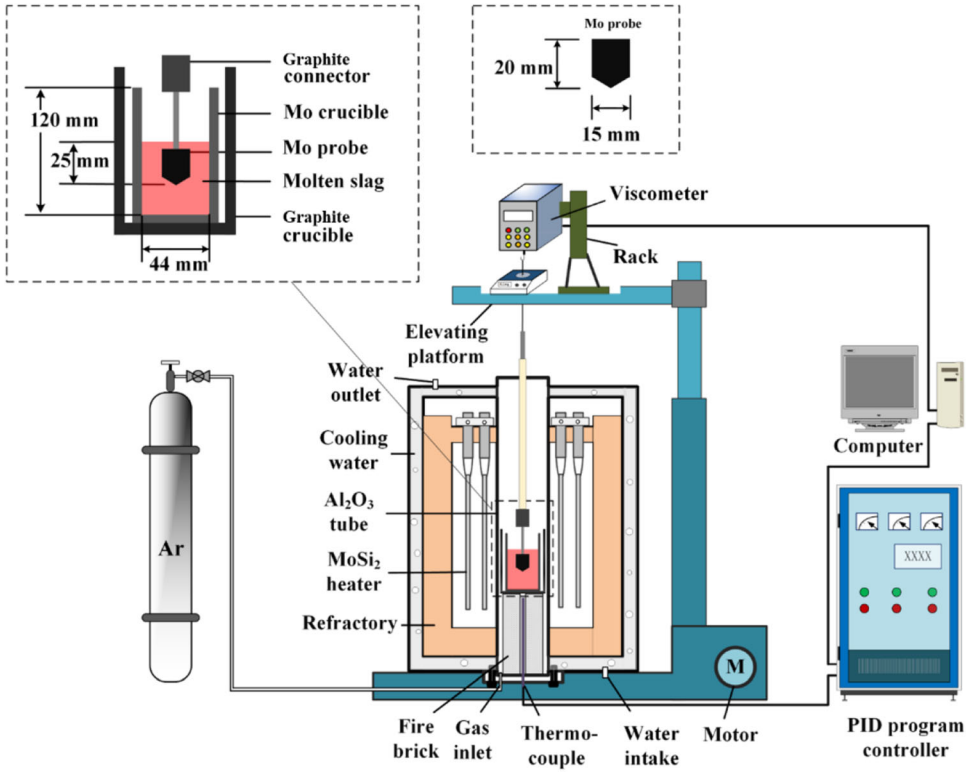

Fig. 1 Schematic diagram of viscosity measurement system

results. After completing the viscosity measurements, the slag samples were reheated to 1550 °C and quenched on a water-cooled plate for further analysis by Raman spectroscopy. Two groups of the quenched slag and the slag after viscosity measurement were verified by chemical analysis. The results showed that the slag composition remained unchanged, which satisfied the requirement of the experiment.

3 Results and discussion

3.1 Effect of Al_2O_3 content on viscosity

In the phase diagram calculated by FactSage 6.2 (Fig. 2), different red lines represent the liquid regions at 1550 °C, 1500 °C, and 1450 °C. Each dot describes the composition location of the slag sample presented in Table 2. Figure 2 shows that the slag samples, except slags 1, 2, 5, and 6, exhibited a mixture of liquid and solid phases at 1550 °C.

Figure 3 shows the relationship between the temperature and the volume percentage of the solid phases in the mixture. The mass fraction of the solid particles was calculated by FactSage 6.2, which is shown in Table 3, as well as the compositions of the liquid and solid phases. Based on the calculated results, the solid slag mainly consists of Mg_2SiO_4 and a small amount of Fe_2SiO_4. The densities of Mg_2SiO_4 and Fe_2SiO_4 obtained by FactSage 6.2 are 3.22 and 4.40 g cm^{-3}, respectively. The density of the liquid slag was obtained using the Mills model based on the liquid slag composition [16].

The volume percentage of all the solid phases (φ) is calculated using the following equations:

$$V_s = M \times W_{s1} \div \rho_{s1} + M \times W_{s2} \div \rho_{s2}, \quad (1)$$

$$V_L = M \times W_L \div \rho_L, \quad (2)$$

$$\varphi = \frac{V_s}{V_s + V_L} = \frac{W_{s1} \div \rho_{s1} + W_{s2} \div \rho_{s2}}{W_{s1} \div \rho_{s1} + W_{s2} \div \rho_{s2} + W_L \div \rho_L}, \quad (3)$$

where M is the mass of the slag, g; V_s is the volume of the solid slag, cm^3; V_L is the volume of liquid slag, cm^3; W_{s1} represents the mass fraction of Mg_2SiO_4, %; W_{s2} represents the mass fraction of Fe_2SiO_4, %; W_L represents the mass fraction of the liquid slag, %; ρ_{s1} is the density of Mg_2SiO_4, g cm^{-3}; ρ_{s2} is the density of Fe_2SiO_4, g cm^{-3}; and ρ_L is the density of the liquid slag, g cm^{-3}. It is well known that the viscosity of partially molten materials or solid suspension liquids is very large. Several models have been used to describe the viscosity of these melts, and the Roscoe model has been widely used [17]. The relative viscosity of a suspension of rigid solid particles is calculated by:

$$\eta_{app} = \eta_{liq}(1 - 1.35\varphi)^{-2.5}, \quad (4)$$

where η_{liq} is the viscosity of the pure liquid slag that eliminates the influence of the solid particles, Pa s; and η_{app} is the apparent viscosity of the slag, Pa s. According to Eq. (4), the viscosity of the pure liquid slag can be obtained.

Figure 4 graphically represents the viscosity of the SiO_2–MgO–FeO–Al_2O_3–CaO-based slag with Al_2O_3 additions and a constant basicity of 1.0 at various temperatures. In Fig. 4, two types of viscosities can be observed. The solid lines express the apparent viscosity, and the dashed lines represent the viscosity of the pure liquid slag that removes the influence of the solid particles.

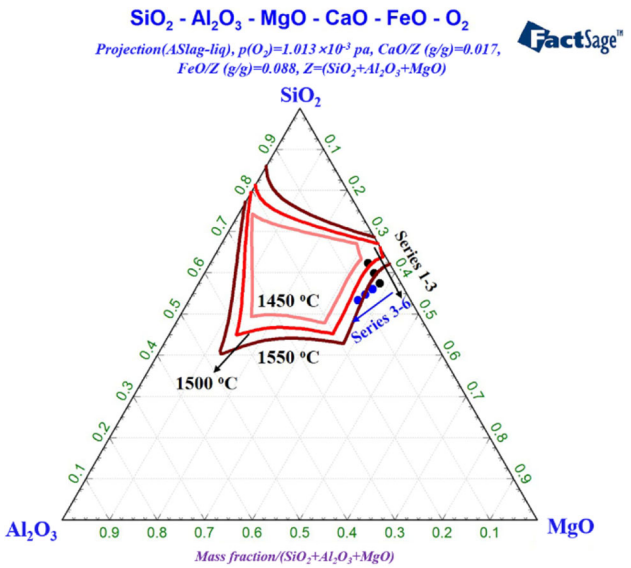

Fig. 2 Phase diagram of SiO_2-MgO-FeO-Al_2O_3-CaO slag

Table 3 Mass fraction of solid slag (%)

Temperature/°C	Slag 1	Slag 2	Slag 3	Slag 4	Slag 5	Slag 6
1470	3.42	15.15	26.24	22.94	18.80	14.45
1480	1.30	13.23	24.51	21.09	16.83	12.34
1490	0.00	11.24	22.72	19.18	14.78	10.15
1500	0.00	9.19	20.88	17.20	12.66	7.88
1510	0.00	7.06	18.97	15.15	10.46	5.52
1520	0.00	4.86	16.98	13.03	8.18	3.06
1530	0.00	2.58	14.92	10.82	5.81	0.50
1540	0.00	0.20	12.77	8.52	3.33	0.00
1550	0.00	0.00	10.54	6.12	0.00	0.00

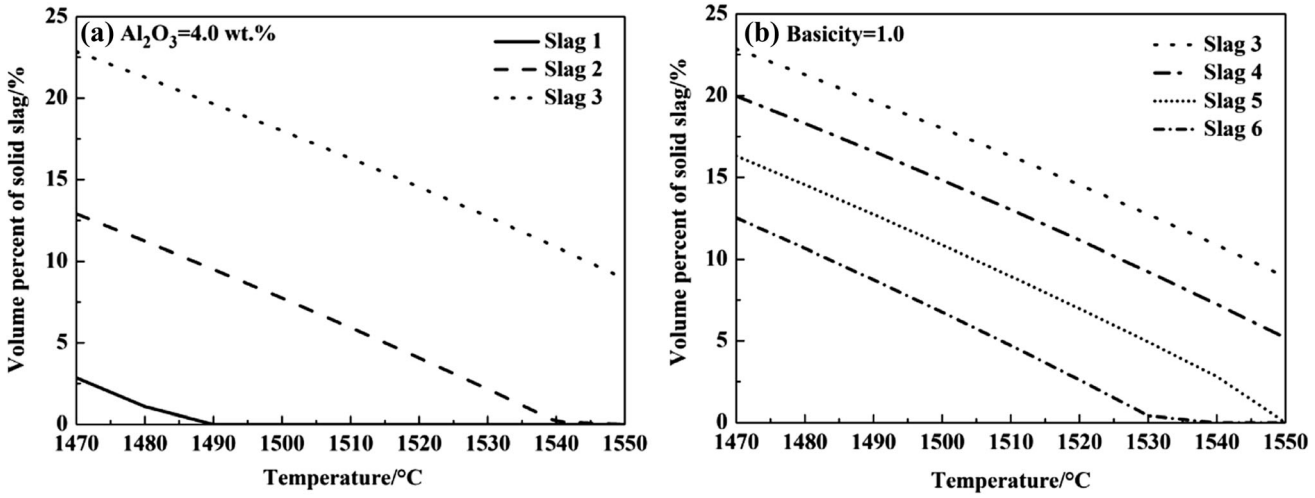

Fig. 3 Relationship between temperature and volume percent of solid slag

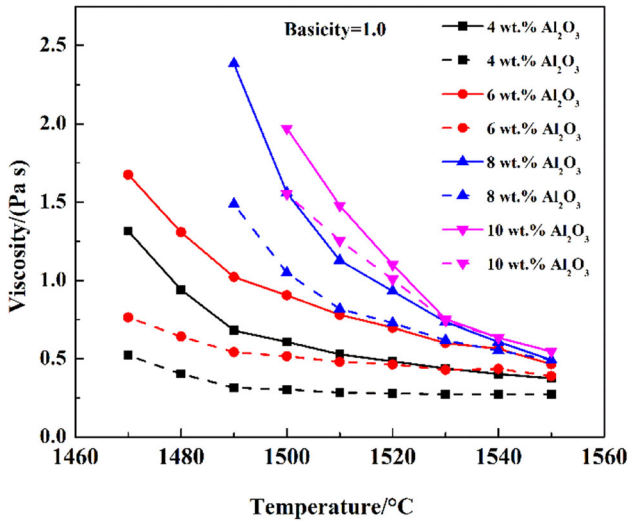

Fig. 4 Effect of Al_2O_3 content on viscosity

Similarly, increasing the Al_2O_3 content increased both the apparent viscosity and the pure liquid viscosity, indicating that Al_2O_3 acts as a network former in this slag system. However, this conclusion still requires much detailed information about the structure to verify it, which will be discussed later. In addition, the apparent viscosities of the slags were higher than the viscosity that does not consider the particles due to the presence of solid particles.

3.2 Effect of basicity on viscosity

The effect of basicity on the viscosity while keeping the sum of MgO and SiO_2 contents constant was investigated and is shown in Fig. 5.

In Fig. 5, two types of viscosities can be observed. The solid lines express the apparent viscosity, and the dashed lines represent the viscosity of the pure liquid slag that eliminates the influence of the solid particles. The slag was in a pure liquid phase when the basicity was 0.8, and therefore, only the pure liquid viscosity is shown in Fig. 5. Similarly, it can be observed that the two types of viscosities decreased as the basicity increased. Basic oxides, such as MgO and CaO, can influence the viscosity indirectly by influencing the aluminosilicate network structure. The observation in Fig. 5 indicates that a relatively high MgO content depolymerizes the slag structure and decreases the slag viscosity by providing additional free oxygen ions (O^{2-}) [18–20].

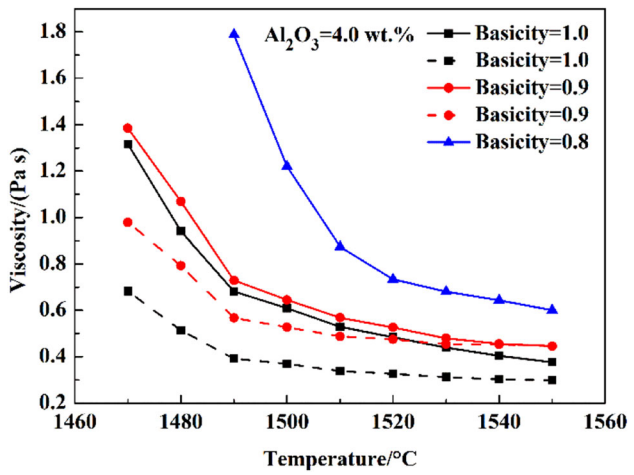

Fig. 5 Effect of basicity on viscosity

3.3 Structural analysis by Raman spectroscopy

Raman spectroscopy is widely accepted as an instrumental technique for determining silicate structures. The characteristic vibration frequencies of the silicate and aluminate structures can be identified by performing Raman spectroscopy. Recently, Mysen et al. [19, 21, 22], McMillan et al. [23–25], and other groups [26–28] systematically determined and utilized the characteristic band intensities of silicate structures to semiquantitatively identify the complex slag structures as detailed in Table 4.

Since slags 1, 2, 5, and 6 were in pure liquid phases at 1550 °C, the Raman spectroscopy was used to analyze the slag structures of slags 1, 2, 5, and 6. A part of the Raman spectra at various Al_2O_3 contents and basicities for specific vibrations of the silicate and aluminate structural units is shown in Fig. 6, in which no significant trough of aluminate structural units was found due to the low Al_2O_3 content in slags 1, 2, 5, and 6.

The integrated area of the individual deconvoluted peaks allows for the semiquantitative evaluation of the amount of characteristic structural units available in the molten slag. The ratio of the integrated area of an individual characteristic structural unit over the sum of the integrated area of all the characteristic structural units provides the fraction of structural units present in the melt. The deconvolution of the Raman spectra at various basicities for specific vibrations of the silicate structural units is shown in Fig. 7. From the integration of the deconvoluted spectra of the various structural units, the fraction of the characteristic structural units in slags 1 and 2 is presented as a function of the basicity in Table 5. The sum of the structural units in slags 1 and 2 of NBO/Si = 4(Q^0) and NBO/Si = 3(Q^1) clearly decreased and that of NBO/Si = 2(Q^2) and NBO/Si = 1(Q^3) increased as the basicity increased. This result suggests that MgO breaks the [SiO_4]–tetrahedra network structure, reduces the polymerization degree of the slag, and forms simple melts. This result agrees well with the viscosity measurement.

The deconvolution of the Raman spectra at various Al_2O_3 contents for specific vibrations of the silicate

Table 4 Raman active spectra vibrations for various structural units

Structural unit	NBO/Si(Q^n)	Wavenumber/cm^{-1}	Vibrational mode
Al–O–Si	–	820–850	Stretching Al–O–Si vibration
$[SiO_4]^{4-}$	4(Q^0)	850–880	Symmetric Si–O^- stretching vibration
$[Si_2O_7]^{6-}$	3(Q^1)	900–920	Symmetric Si–O^- stretching vibration
$[SiO_3]^{2-}$	2(Q^2)	950–980	Symmetric Si–O^- stretching vibration
$[Si_2O_5]^{2-}$	1(Q^3)	1050–1150	Symmetric Si–O^- stretching vibration

NBO Non-bridging oxygen

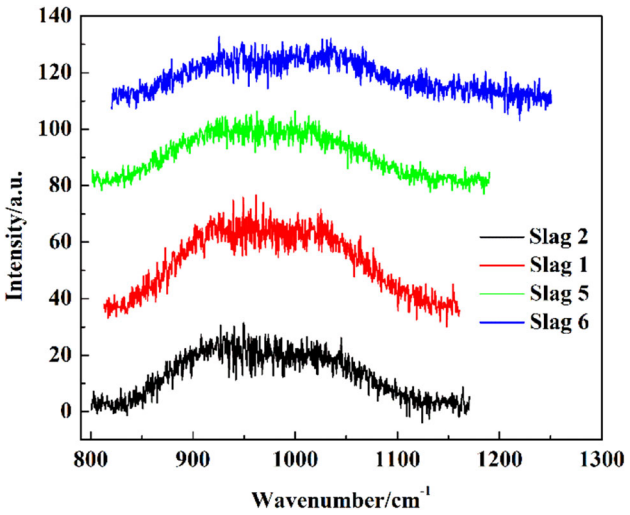

Fig. 6 Raman spectra of parts of as-quenched samples of slags 1, 2, 5, and 6

structural units is shown in Fig. 8. From the integration of the deconvoluted spectra of the various structural units, the fraction of the characteristic structural units in slags 5 and 6 is presented as a function of the Al_2O_3 content in Table 6.

Table 5 Fractions of various structural units in slags 1 and 2 (%)

Structural unit	Slag 1	Slag 2
NBO/Si = 1 (Q^3)	28.49	51.54
NBO/Si = 2 (Q^2)	5.80	7.54
NBO/Si = 3 (Q^1)	64.86	33.87
NBO/Si = 4 (Q^0)	0.85	7.05
NBO/Si = 1 + 2	34.29	59.08
NBO/Si = 3 + 4	65.71	40.92

As shown in Table 6, the sum of the structural units of NBO/Si = 1(Q^3) and NBO/Si = 2(Q^2) slightly decreased and that of NBO/Si = 3(Q^1) and NBO/Si = 4(Q^0) increased as the Al_2O_3 content increased. This result indicates that Al_2O_3 acts as a network former in this slag system, making the slag structure complex, and this result corresponds well with the viscosity measurement.

4 Conclusions

1. The slag viscosity was measured from 1450 to 1550 °C using the rotating cylindrical method. The results

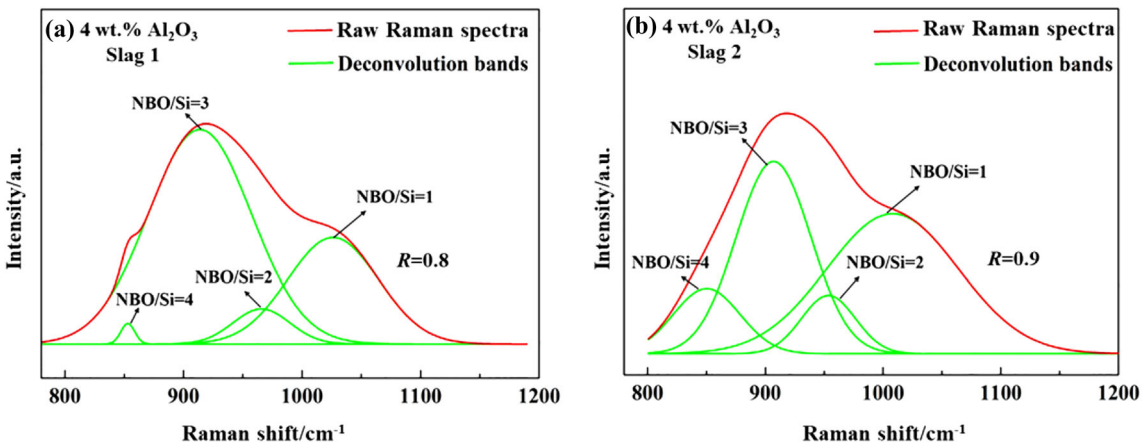

Fig. 7 Deconvoluted results of Raman spectra curves of slags 1 and 2

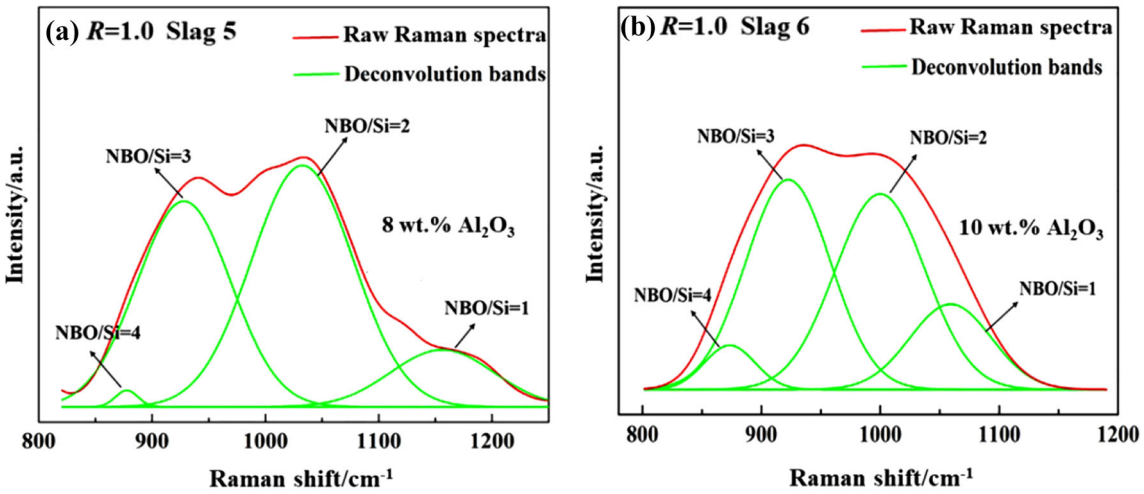

Fig. 8 Deconvoluted results of Raman spectra curves of slags 5 and 6

Table 6 Fractions of various structural units in slags 5 and 6 (%)

Structural unit	Slag 5	Slag 6
NBO/Si = 1 (Q^3)	9.71	15.60
NBO/Si = 2 (Q^2)	51.38	39.92
NBO/Si = 3 (Q^1)	38.09	39.45
NBO/Si = 4 (Q^0)	0.82	5.03
NBO/Si = 1 + 2	61.09	55.52
NBO/Si = 3 + 4	38.91	44.48

showed that the slag was a mixture of liquid and solid phases under the experimental temperature.

2. The viscosity decreases as the basicity increases and increases as the Al_2O_3 content increases.
3. MgO is likely to depolymerize the slag structure into simple polymer-type units, thereby increasing viscosity. Al_2O_3 acts as a network former in the slag system, thereby making the slag structure additionally complex and increasing the viscosity.

Acknowledgements The authors are especially grateful to the National Natural Science Foundation of China (Grant No. 51234010) and the Fundamental Research Funds for the Central Universities (Project Nos. 2018CDXYCL0018 and 2018CDPTCG0001/11) for the financial support of this research.

References

[1] M.G. King, JOM 57 (2005) 35–39.
[2] A.E.M. Warner, C.M. Díaz, A.D. Dalvi, P.J. Mackey, A.V. Tarasov, JOM 58 (2006) 11–20.
[3] M. Liu, X.W. Lv, E.G. Guo, P. Chen, Q.G. Yuan, ISIJ Int. 54 (2014) 1749–1754.
[4] G.M. Mudd, Ore Geol. Rev. 38 (2010) 9–26.
[5] J.B. Chen, J.H. Xu, Modern Mining 25 (2006) No. 8, 1–3.
[6] S.W. Zhang, S.B. Xie, A.D. Xu, World Nonferrous Met. 11 (2003) 9–14.
[7] X.W. Lv, C.G. Bai, S.P. He, Q.Y. Huang, ISIJ Int. 50 (2010) 380–385.
[8] C. Pan, C.G. Bai, X.W. Lv, L.M. Hu, T. Hu, Metal. Int. 16 (2011) 5–9.
[9] E.N. Zevgolis, C. Zografidis, T. Perraki, E. Devlin, J. Therm. Anal. Calorim. 100 (2010) 133–139.
[10] I. Kobayashi, Y. Tanigaki, A. Uragami, Iron Steelmaker 28 (2001) No. 9, 19–22.
[11] Z.H. Liu, X.B. Ma, D.Q. Zhu, Y.H. Li, Q.H. Li, J. Cent. South Univ. (Sci. Technol.) 42 (2011) 2905–2910.
[12] G.B. Qiu, L. Chen, J.Y. Zhu, X.W. Lv, C.G. Bai, ISIJ Int. 55 (2015) 1367–1376.
[13] P. McMillan, Am. Miner. 69 (1984) 622–644.
[14] K. Zheng, J. Liao, X. Wang, Z. Zhang, J. Non-Cryst. Solids 376 (2013) 209–215.
[15] J.H. Park, Metall. Mater. Trans. B 44 (2013) 938–947.
[16] K.C. Mills, S. Sridhar, Ironmak. Steelmak. 26 (1999) 262–268.
[17] R. Roscoe, Br. J. Appl. Phys. 3 (1952) 267–269.
[18] H. Park, J.Y. Park, G.H. Kim, I. Sohn, Steel Res. Int. 83 (2012) 150–156.
[19] B.O. Mysen, Earth Sci. Rev. 27 (1990) 281–365.
[20] A. Fernández-Jiménez, F. Puertas, I. Sobrados, J. Sanz, J. Am. Ceram. Soc. 86 (2003) 1389–1394.
[21] B.O. Mysen, L.W. Finger, D. Virgo, F.A. Seifert, Am. Miner. 67 (1982) 686–695.
[22] B.O. Mysen, D. Virgo, F.A. Seifert, Rev. Geophys. 20 (1982) 353–383.
[23] P. McMillan, B. Piriou, J. Non-Cryst. Solids 55 (1983) 221–242.
[24] P.F. McMillan, B.T. Poe, P.H. Gillet, B. Reynard, Geochim. Cosmochim. Acta 58 (1994) 3653–3664.
[25] P. McMillan, B. Piriou, A. Navrotsky, Geochim. Cosmochim. Acta 46 (1982) 2021–2037.
[26] V.N. Bykov, A.A. Osipov, V.N. Anfilogov, Glass Phys. Chem. 29 (2003) 105–107.
[27] C. Huang, E.C. Behrman, J. Non-Cryst. Solids 128 (1991) 310–321.
[28] I. Daniel, P. Gillet, B.T. Poe, P.F. McMillan, Phys. Chem. Miner. 22 (1995) 74–86.